Figure S1

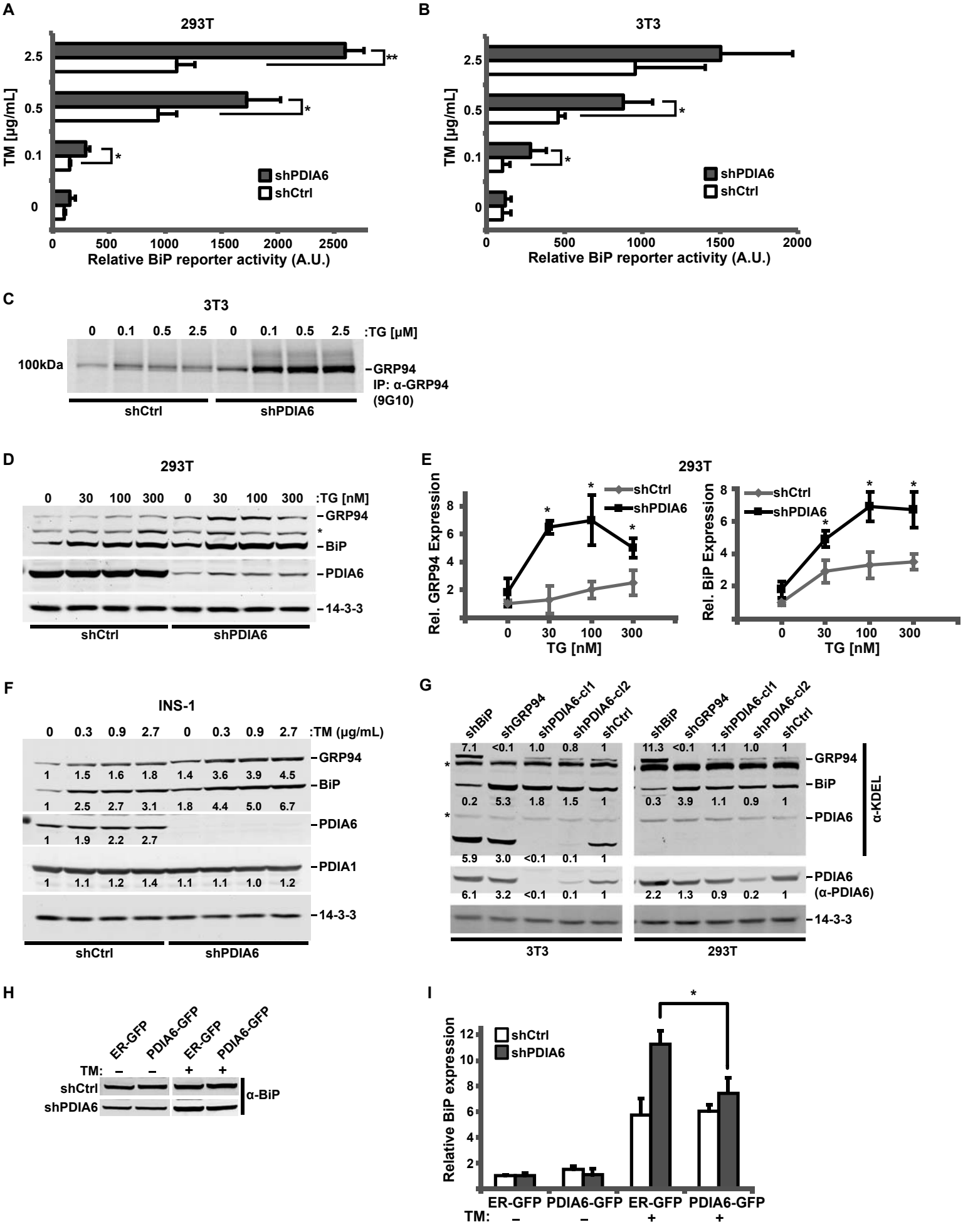
A
293T
TM [μg/mL]
2.5
0.5
0.1
0
shPDIA6
shCtrl
0
500
1000
1500
2000
2500
Relative BiP reporter activity (A.U.)
B
3T3
TM [μg/mL]
2.5
0.5
0.1
0
shPDIA6
shCtrl
0
500
1000
1500
2000
Relative BiP reporter activity (A.U.)
C
3T3
0 0.1 0.5 2.5 0 0.1 0.5 2.5 :TG [μM]
100kDa
GRP94
IP: α-GRP94
(9G10)
shCtrl
shPDIA6
D
293T
0 30 100 300 0 30 100 300 :TG [nM]
GRP94
*
BiP
PDIA6
14-3-3
shCtrl
shPDIA6
E
293T
Rel. GRP94 Expression
shCtrl
shPDIA6
0 30 100 300
TG [nM]
Rel. BiP Expression
shCtrl
shPDIA6
0 30 100 300
TG [nM]
F
INS-1
0 0.3 0.9 2.7 0 0.3 0.9 2.7 :TM (μg/mL)
GRP94
1 1.5 1.6 1.8 1.4 3.6 3.9 4.5
BiP
1 2.5 2.7 3.1 1.8 4.4 5.0 6.7
PDIA6
1 1.9 2.2 2.7
PDIA1
1 1.1 1.2 1.4 1.1 1.1 1.0 1.2
14-3-3
shCtrl
shPDIA6
G
shBiP shGRP94 shPDIA6-cl1 shPDIA6-cl2 shCtrl
7.1 <0.1 1.0 0.8 1
0.2 5.3 1.8 1.5 1
5.9 3.0 <0.1 0.1 1
6.1 3.2 <0.1 0.1 1
shBiP shGRP94 shPDIA6-cl1 shPDIA6-cl2 shCtrl
11.3 <0.1 1.1 1.0 1
0.3 3.9 1.1 0.9 1
2.2 1.3 0.9 0.2 1
GRP94
BiP
PDIA6
α-KDEL
PDIA6
(α-PDIA6)
14-3-3
3T3
293T
H
ER-GFP PDIA6-GFP ER-GFP PDIA6-GFP
TM: – – + +
shCtrl
shPDIA6
α-BiP
I
Relative BiP expression
12
10
8
6
4
2
shCtrl
shPDIA6
ER-GFP PDIA6-GFP ER-GFP PDIA6-GFP
TM: – – + +

Figure S1, related to Figure 1.

The augmented responsiveness to ER stress by PDIA6 depletion is not cell specific.

This figure shows additional evidence of the hyper-responsiveness phenotype due to PDIA6 silencing.

(A) The transcriptional activity of BiP promoter is enhanced in 293T cells depleted for PDIA6, upon ER stress. shCtrl or shPDIA6 (clone 3) 293T cells transiently expressing luciferase driven by the minimal promoter of BiP (Eletto et al., 2012) were treated with the indicated doses of TM. 18 hrs later, cell lysates were assayed for both firefly and Renilla luciferase activities. The raw data were normalized to Renilla activity and shown as means±SD in arbitrary units (A.U.) (n=4). The same cells silenced with the same shPDIA6 clone were also used in the proliferation assay shown in Fig. 2C.

(B). shCtrl or shPDIA6 (clone 1) 3T3 cells were assayed for BiP promoter activity as in **A**. (*, $p \leq 0.05$; **, $p \leq 0.01$).

(C) Autoradiogram of the gel used to analyse the metabolic labeling GPR94, whose quantification is shown in Fig. 1C.

(D-E) Human 293T cells stably expressing shCtrl or shPDIA6 (clone 3) were treated with the indicated concentrations of TG for 16 hrs and analysed as in Fig 1D-E. The quantification in E is based on 3 independent experiments (*, $p \leq 0.05$).

(F) Akita-INS cells, stably expressing shCtrl or shPDIA6 (clone 1), were stressed with the indicated doses of TM for 18 hrs, without Dox induction. Protein extracts were analysed by immunoblotting as in Fig. 1D-E. Expression levels of the indicated proteins normalized to shCtrl, untreated cells are denoted under the respective bands.

(G) Silencing of BiP, GRP94 and PDIA6 in murine 3T3 and human 293T cells with lentiviral shRNA vectors (Eletto et al., 2012). Protein extracts from cells stably expressing the indicated shRNA clones, were analysed by immunoblotting to determine the level of expression of GRP94, BiP and PDIA6. Since human PDIA6 is not detectable by the α-KDEL antibody (Eletto et al., 2012), blots were also probed with a specific α-PDIA6 antibody. Fold induction (indicated near each band) was calculated by band densitometry normalized to the loading control, 14-3-3, which was then compared to the values from the shCtrl samples. *, non-specific bands detected by α-KDEL. Note that the same phenotype is observed with two distinct shRNA sequences for either 3T3 or 293T cells. Both GRP94 and BiP are robustly induced when the other is depleted (BiP is induced by 4-5 fold; GRP94 by 7-11 fold in 3T3 and 293T cells). In comparison, limiting PDIA6 causes either a modest (in 3T3 cells) or negligible response (in 293T), even when the silencing is complete.

(H) The hyper-response of PDIA6-depleted 293T cells to 2μg/mL TM for 24hrs was used as a read-out for a complementation test. Briefly, shCtrl and shPDIA6-cells (clone 2) were transiently transfected with either ER-GFP (ER-localized GFP) or PDIA6-GFP and then subjected to TM or left in growth medium. The levels of BiP expression were determined by immunoblots.

(I) The relative expression of BiP in PDIA6-sufficient and PDIA6-defficient cells, expressing the exogenous constructs as in **H**. Values were normalized to BiP level in untransfected and non-stressed cells. Bars are means±SD (n = 3; *, p-value ≤ 0.05).

Figure S2

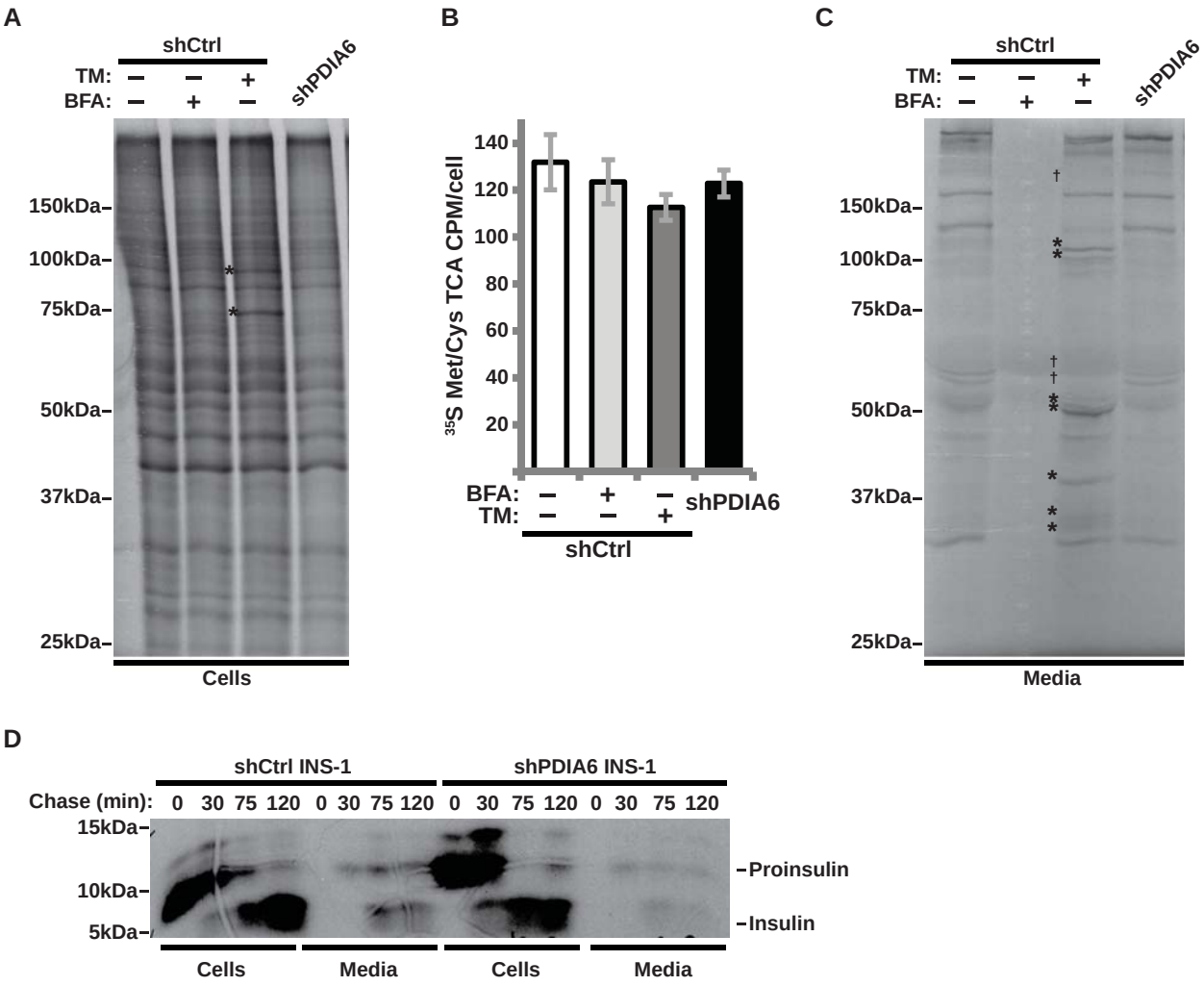
A
shCtrl
shPDIA6
TM:
BFA:
150kDa
100kDa
75kDa
50kDa
37kDa
25kDa
Cells
B
35S Met/Cys TCA CPM/cell
140
120
100
80
60
40
20
BFA:
TM:
shPDIA6
shCtrl
C
shCtrl
shPDIA6
TM:
BFA:
150kDa
100kDa
75kDa
50kDa
37kDa
25kDa
Media
D
shCtrl INS-1
shPDIA6 INS-1
Chase (min): 0 30 75 120 0 30 75 120 0 30 75 120 0 30 75 120
15kDa
10kDa
5kDa
Proinsulin
Insulin
Cells
Media
Cells
Media

Figure S2, related to Figure 1 and 2.

Loss of PDIA6 does not cause aberration in protein synthesis or secretion.

This figure shows that PDIA6 plays a negligible role in protein folding and secretion. Hence, the augmented susceptibility to ER stress in PDIA6-depleted cells cannot be ascribed to accumulation of misfolded substrates.

(A, C) 293T cells stably expressing shCtrl or shPDIA6 (clone 3) were pulse labeled with [^{35}S]Met/Cys for 4hrs. Cell lysates (A) and culture supernatants (C) were harvested and analysed by SDS-PAGE. Treatments with brefeldin A (BFA, 3μg/mL, added 30min before the pulse) or TM (10μg/mL added 3hrs prior the labeling) served as controls for protein secretion and folding, respectively. Note the new (*) or lost (†) secreted species upon TM treatment (panel C). Note also BiP and GRP94 in the cell lysates (*, panel A).

(B) Quantitation of protein synthesis under the indicated conditions/drug treatments. Plotted are means±SD of TCA-precipitable [^{35}S]Met/Cys counts per cell, incorporated during a 30 min period (n=2). The normal protein synthesis in PDIA6-depleted cells stands in contrast to the ~50% inhibition of protein synthesis when BiP is depleted (Eletto et al., 2012).

(D) INS-1 832/13 β-cells were transduced with shCtrl or shPDIA6 lentiviruses, metabolically labeled for 30 min and then chased for the indicated times. Cell lysates and culture supernatants were harvested for immunoprecipitation of radiolabeled proinsulin/insulin, which were resolved by urea/acrylamide gels optimized for small proteins, followed by autoradiography.

Figure S3

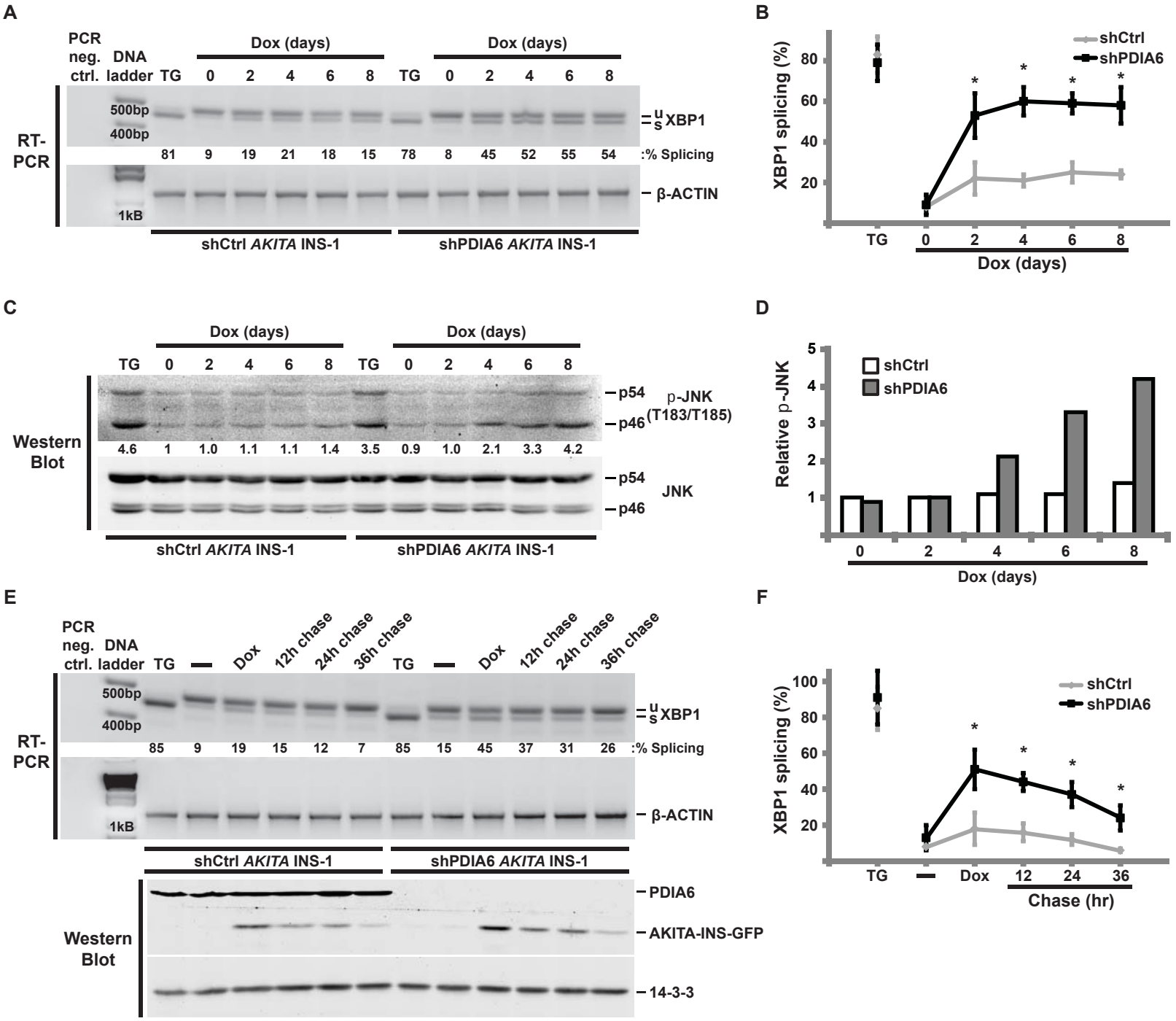
A
PCR neg. ctrl.
DNA ladder
Dox (days)
TG 0 2 4 6 8 TG 0 2 4 6 8
500bp
400bp
RT-PCR
u
s XBP1
81 9 19 21 18 15 78 8 45 52 55 54 :% Splicing
1kB
β-ACTIN
shCtrl AKITA INS-1
shPDIA6 AKITA INS-1
B
XBP1 splicing (%)
shCtrl
shPDIA6
TG 0 2 4 6 8
Dox (days)
C
Dox (days)
TG 0 2 4 6 8 TG 0 2 4 6 8
Western Blot
p54
p46
p-JNK (T183/T185)
4.6 1 1.0 1.1 1.1 1.4 3.5 0.9 1.0 2.1 3.3 4.2
JNK
shCtrl AKITA INS-1
shPDIA6 AKITA INS-1
D
Relative p-JNK
shCtrl
shPDIA6
0 2 4 6 8
Dox (days)
E
PCR neg. ctrl.
DNA ladder
TG — Dox 12h chase 24h chase 36h chase TG — Dox 12h chase 24h chase 36h chase
500bp
400bp
RT-PCR
u
s XBP1
85 9 19 15 12 7 85 15 45 37 31 26 :% Splicing
1kB
β-ACTIN
shCtrl AKITA INS-1
shPDIA6 AKITA INS-1
Western Blot
PDIA6
AKITA-INS-GFP
14-3-3
F
XBP1 splicing (%)
shCtrl
shPDIA6
TG — Dox 12 24 36
Chase (hr)

Figure S3, related to Figure 3.

PDIA6 silencing leads to augmented IRE1 signaling in response to Akita mutant.

This figure complements Figure 3 by showing that loss of PDIA6 prolongs XBP1 splicing in response to the stress of expressing the mutant Akita insulin.

(A) RNA samples from either shCtrl or shPDIA6 Akita-INS clones. Cells from each clone were induced with Dox for up to eight days and assayed for XBP1 splicing. u, unspliced XBP1; s, spliced XBP1.

(B) Quantitation of three RT-PCR experiments as in **A**. Plotted are means of percentage of XBP1 splicing ± SD. (*, p-value ≤ 0.05).

(C) Immunoblots of the same cells to show levels of JNK and phospho-JNK at different times of Dox induction.

(D) Relative phospho-JNK values from panel C. Phospho-JNK/total JNK ratios from each time point were normalized to the uninduced shCtrl sample.

(E-F) Analysis of the same clones as in **A** using a pulse-chase regime. The cells were "pulsed" with Dox for 2 days, followed by "chase" in medium without Dox for 12, 24 or 36hr. XBP1 splicing, immunoblots and quantitation were performed as in **A-B**.

Figure S4

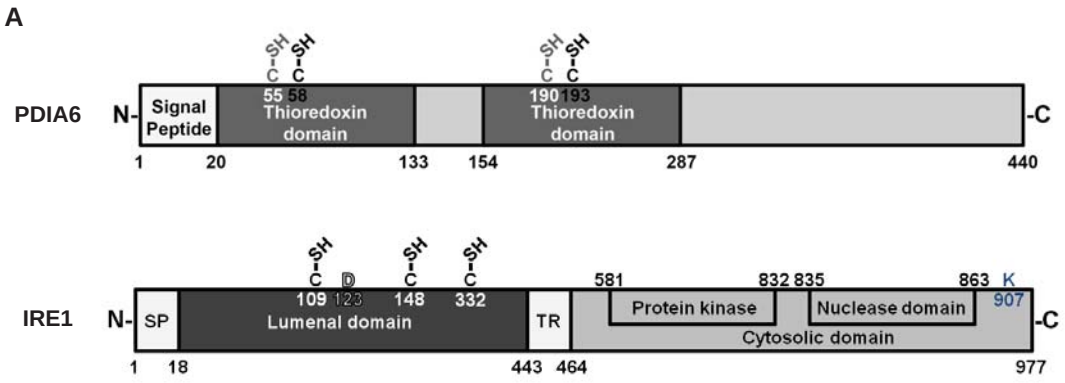
A
PDIA6
N-
Signal Peptide
SH C SH C
55 58
Thioredoxin domain
SH C SH C
190 193
Thioredoxin domain
-C
1
20
133
154
287
440
IRE1
N-
SP
SH C
109
D
123
SH C
148
SH C
332
Lumenal domain
TR
581
832 835
Protein kinase
Nuclease domain
863 K
907
Cytosolic domain
-C
1
18
443
464
977

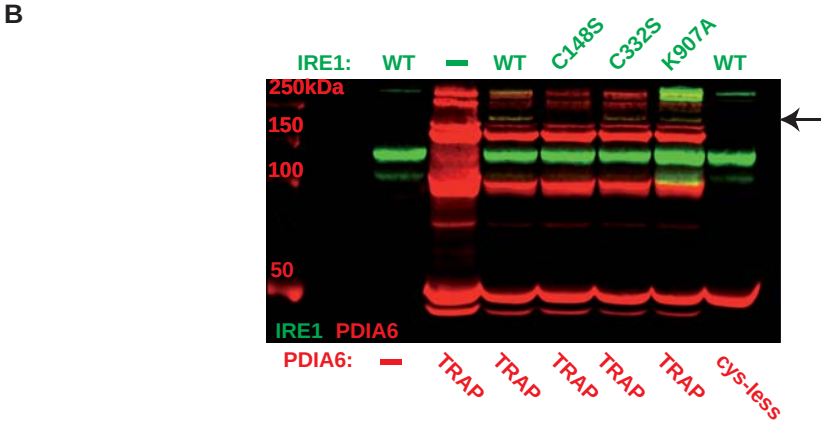
B
IRE1: WT – WT C148S C332S K907A WT
250kDa
150
100
50
IRE1 PDIA6
PDIA6: – TRAP TRAP TRAP TRAP TRAP cys-less

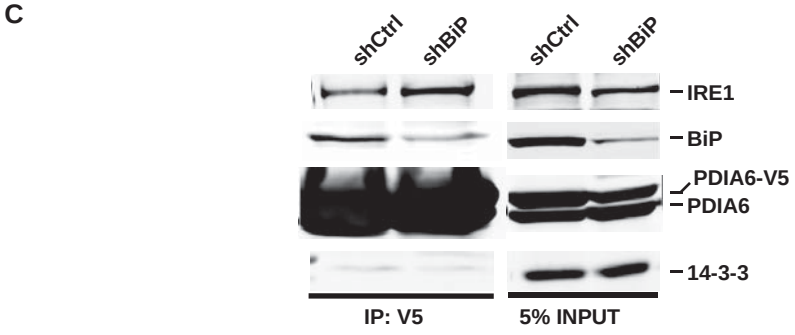
C
shCtrl
shBiP
shCtrl
shBiP
IRE1
BiP
PDIA6-V5
PDIA6
14-3-3
IP: V5
5% INPUT

Figure S4, related to Figures 3 and 4.

PDIA6 binding to IRE1 is dependent on Cys and independent of BiP.

The data here extend the mechanistic details about the physical interaction between PDIA6 and IRE1. This figure also provides schematic diagrams of the proteins.

(A) Dual color blot of the interaction experiment shown in Fig. 4F. Arrow, the mixed disulfide species of IRE1 and PDIA6 (yellow).

(B) 293T cells, stably expressing non-targeting (shCtrl) or BiP-targeting shRNA, were transfected with the trapping mutant of PDIA6-V5, lysed and subjected to immunoprecipitation with α-V5. Samples were then analysed by Western blot to detect the associated IRE1. 14-3-3 served as negative control of co-IP.

(C) Block diagrams of PDIA6 and IRE1 proteins highlighting the cysteines relevant for their interaction. SP, signal peptide; TR, trans-membrane region. In PDIA6, the cysteines in black were mutated to create the trap mutant, while all four were mutated to create the Cys-less mutant.

Figure S5

A

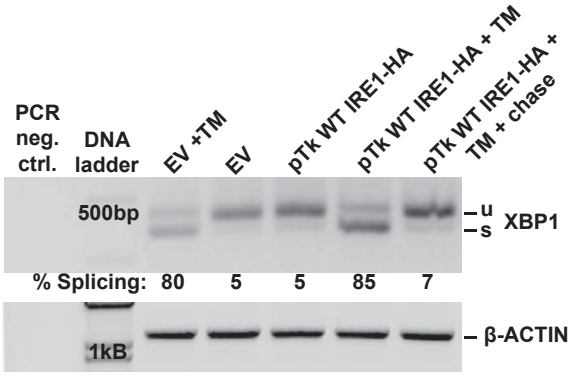
PCR neg. ctrl.
DNA ladder
EV +TM
EV
pTk WT IRE1-HA
pTk WT IRE1-HA + TM
pTk WT IRE1-HA + TM + chase
500bp
u
s
XBP1
% Splicing: 80 5 5 85 7
1kB
β-ACTIN

B

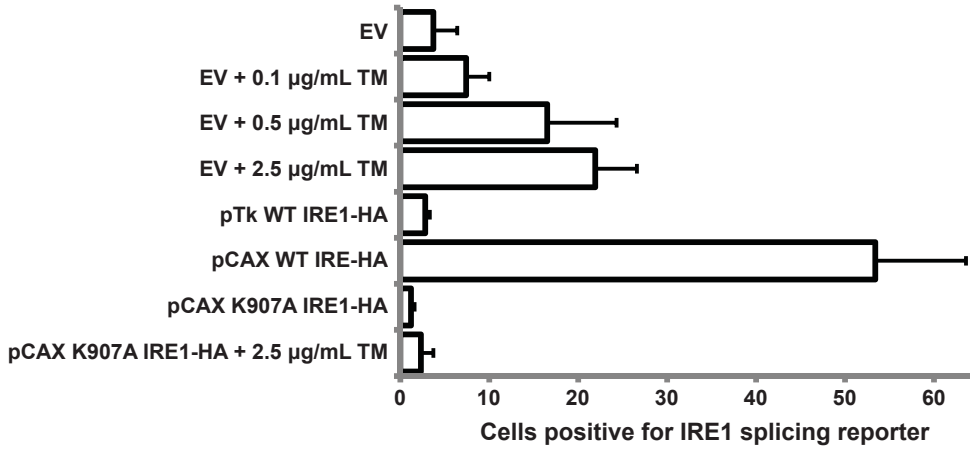
EV
EV + 0.1 µg/mL TM
EV + 0.5 µg/mL TM
EV + 2.5 µg/mL TM
pTk WT IRE1-HA
pCAX WT IRE-HA
pCAX K907A IRE1-HA
pCAX K907A IRE1-HA + 2.5 µg/mL TM
0
10
20
30
40
50
60
Cells positive for IRE1 splicing reporter

Figure S5, related to Figure 5.

XBP1 splicing activity of various IRE1 constructs

It shows the splicing activity of individual IRE1 constructs. Data were generated by RT-PCR-based XBP1 splicing or fluorescent reporter analysis.

(A) XBP1 splicing assay on 293T cells expressing the indicated IRE1 constructs. 2μg/ml TM for 3 hours induced robust XBP1 splicing, whereas mere expression of WT IRE1-HA driven by the weak TK promoter did not. Proper activation/inactivation of IRE1 was observed when WT IRE1-HA expressing cells were exposed to TM and then chased for 24 hours in fresh medium.

(B) A fluorescence reporter assay for XBP1 splicing was used as a readout of the ER stress response. The reporter was a modified version of the one described in (Rutkowski et al., 2006), where expression of Tomato fluorescent protein was dependent on splicing of the XBP1 intron. 293T cells, transiently expressing the reporter, were treated as indicated, imaged by fluorescence microscopy and the number of reporter-positive cells per field (from 10-15 fields) was enumerated with the Volocity software. pCAX, cytomegalovirus enhancer and chicken β-actin promoter driving over-expression of HA-tagged IRE1; K907, an RNase-deficient mutant of IRE1 expressed like its WT counterpart. Note that mere over-expression of WT IRE1-HA leads to high level splicing, higher even than high TM treatment, while expression from the weak TK promoter mimics endogenous IRE1 activity. The K907A mutant suppresses the stress response of the endogenous IRE1, as previously observed by (Han et al., 2009).

Figure S6

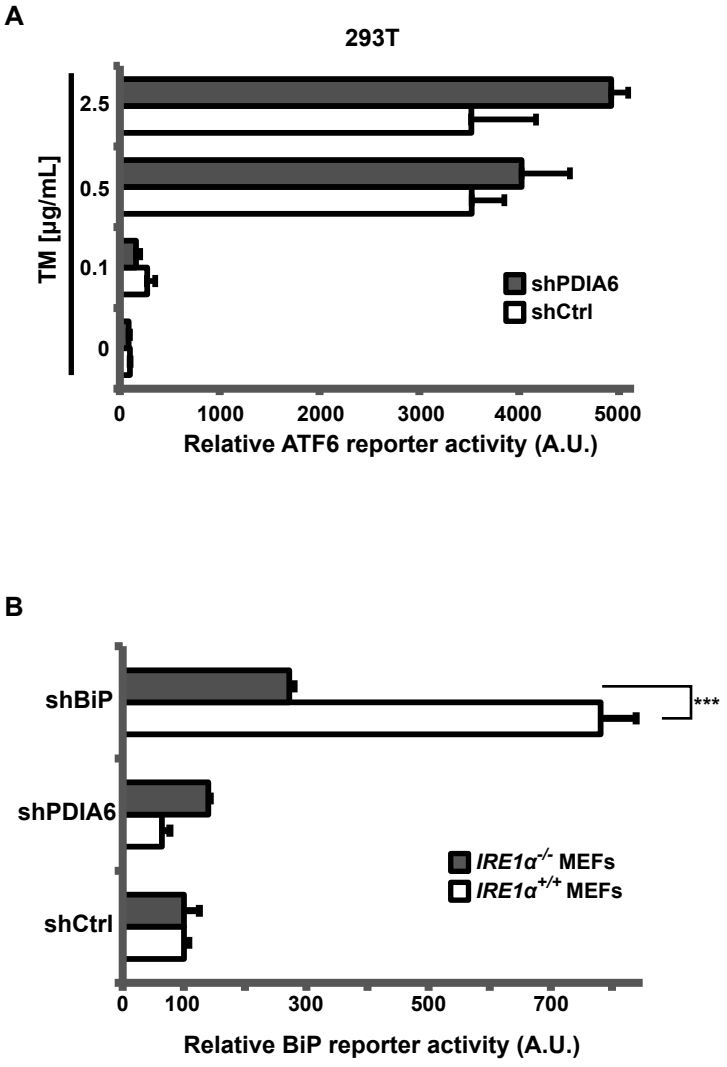
A
293T
TM [μg/mL]
2.5
0.5
0.1
0
shPDIA6
shCtrl
0
1000
2000
3000
4000
5000
Relative ATF6 reporter activity (A.U.)
B
shBiP
shPDIA6
shCtrl
***
IRE1α-/- MEFs
IRE1α+/+ MEFs
0
100
300
500
700
Relative BiP reporter activity (A.U.)

Figure S6, related to Figure 6.

Luciferase reporter analyses of the requirements for the ATF6 and IRE1 UPR branches.

This figure shows an additional analysis of the ATF6 luciferase reporter, in PDIA6-deficient or -sufficient 293T cells. It also shows the transcriptional activity of the BiP promoter in IRE1$\alpha^{-/-}$ or IRE1$\alpha^{+/+}$ MEFs.

(A) shCtrl or shPDIA6 293T cells were transfected with the 5X ATF6 site luciferase reporter, treated with the indicated doses of TM, and assayed for luciferase activity as in Fig. 6D.

(B) Lentiviral transduction was used to deliver shCtrl, shPDIA6 (clone 1) or shBiP into IRE1$\alpha^{+/+}$ or IRE1$\alpha^{-/-}$ MEFs. Cells were then transiently transfected with the luciferase-BiP reporter. 18 hrs later, cell lysates were assayed for firefly and Renilla luciferase activities. The raw data were normalized to Renilla activity, using shCtrl as internal reference for each cell line. Percentages of the means$\pm$SD are plotted (n=3; ***, $p< 0.01$). Altogether, these analyses indicate that silencing of PDIA6 does not cause spontaneous activation of BiP promoter. Moreover, the induction of transcription by silencing BiP itself depends largely on IRE1.

Figure S7

A

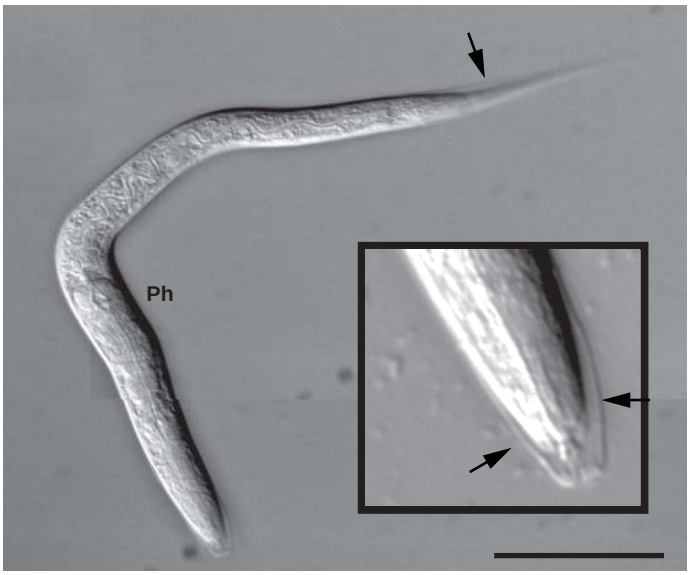

B

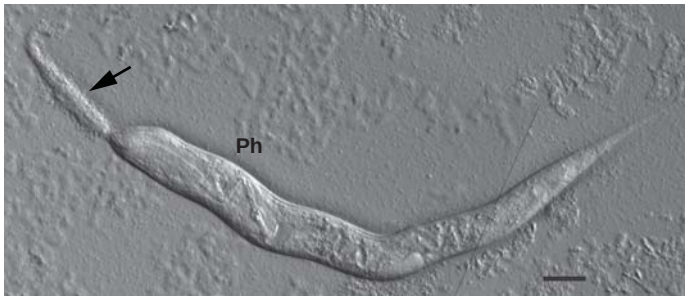

C

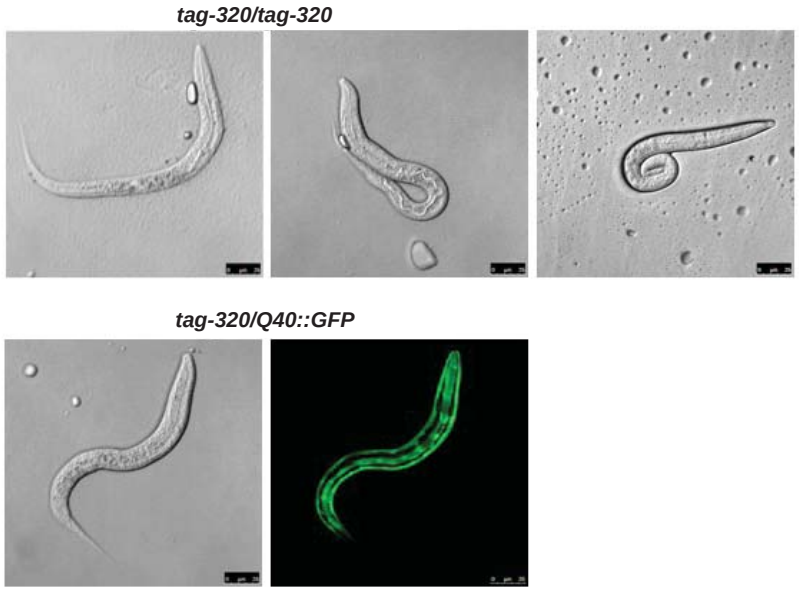

Figure S7, related to Figure 7.

Larval arrest and molting defects in *pdi-6* homozygotes.

This figure shows the larval arrest phenotype and the molting phenotype of *tag-320* deficient animals.

(A) *pdi-6/pdi-6* homozygous larva showing a molting defect, with the vestigial cuticle evident at both ends of the body (arrows). Inset, close-up of the animal head showing the separation of the cuticle (arrows). Larvae are the same age as in Fig. 7C.

(B) *pdi-6/pdi-6* homozygous 3 days-old arrested larva, when the corresponding heterozygotes reach adulthood. Arrow, cuticle remnant protruding from the head. Note the deformed pharynx. Scale bar in A - 50 μm, in B - 5 μm, and in C - 20 μm.

(C) Newly hatched (within 24 hrs) *pdi-6/pdi-6* homozygous larvae appear grossly normal. Top panels, three *pdi-6/pdi-6* homozygous (non-fluorescent) larvae. Bottom panel, a heterozygous larva viewed by both bright field illumination and fluorescence.

Supplemental Experimental Procedures

Tissue culture

3T3 mouse embryonic fibroblasts, 293T human embryonic kidney cells and HeLa human cervical adenocarcinoma cells were all obtained from ATCC and maintained in DMEM (Mediatech) with 10% heat-inactivated fetal bovine serum (Gemini Bio-Product), 100U penicillin, 100U streptomycin and 292μg/mL glutamine (Gibco). A clone of rat pancreatic INS-1 β cells, expressing a doxycyclin-inducible Ins-2(C96)-EGFP fusion protein was kindly provided by Dr. Allen Volchuk (Univ. of Toronto) and maintained as reported in (Hartley et al., 2010). IRE1 knockout (KO) mouse embryonic fibroblasts (MEFs) (Dr. David Ron, Univ. of Cambridge, UK) were maintained as reported in (Urano et al., 2000). IRE1-complemented IRE1 KO MEFs were generated by two consecutive transductions with lentiviral particles carrying pLVX-Tet-On™ or pLVX-Tight-Puro™ plasmids (Clontech). Two days post-infection, cells were cultured in the presence of 3μg/mL puromycin for a week. Pools of transfectants were then induced with 2μg/mL doxycyclin to express IRE1-HA. When required, the following antibiotics were used to select stable cell clones: puromycin (Invivogen), G418 (Gemini) and hygromycin B (Roche). Transient transfections of plasmids were performed using Lipofectamine 2000 (Life Technologies) according to the manufacturer's protocol.

ER stress induction

Throughout this study, chemical ER stress was induced with either TG or TM. The concentration of each and the duration of the treatments were optimized experimentally for each cell line employed here, because the dose that gave rise to modest UPR depended on the cell line and the signaling pathway studied.

Chemicals, plasmids, molecular cloning and mutagenesis

ABT 737 (Bcl2 inhibitor) was from Santa Cruz Biotechnology; doxycycline hydrochloride and MG-132 were from Sigma; TG and TM - from Calbiochem. pcDNA3-PDIA6-V5 plasmid was a kind gift from Dr. Neil Bulleid (Univ. of Glasgow). pTK-basal and pCAX-IRE1-HA constructs were generously provided by Dr. Takao Iwawaki (Gunma University). IRE1-HA cDNA was cloned in pLVX-Tight-Puro vector by PCR. Briefly, pTK-basal-IRE1-HA served as a template to introduce NotI and ECORI restrictions sites at 5' and 3'of the coding sequence, respectively. NLD (amino acids 19-441) IRE1 cDNA was cloned in pcDNA3.1 with a FLAG tag at the N-terminus and a KDEL ER retention signal at the C-terminus. Site-directed mutagenesis using the QuickChange™ kit (Agilent) to generate the following mutants: C58A-C193A PDIA6-V5 trapping mutant; C55A-C58A-C190A-C193A PDIA6-V5 Cysteine-less mutant; K907A IRE1-HA RNAse deficient mutant; D123P IRE1-HA mutant; C109S or C148S or C332S IRE1-HA mutants.

RT-qPCR

For analysis of the relative abundance of transcripts in response to ER stress, 3T3 cells were plated in 60-mm dishes and subjected to TM as indicated. After 6 hrs, total RNA was extracted with TRIzol reagent (Invitrogen) according to the manufacturer's protocol. One microgram of RNA was retrotranscribed into cDNA using random hexamers (SuperScript® II Reverse Transcriptase - Invitrogen). Quantitative PCR was performed using Power SYBR Green mastermix on a StepOne Real-Time PCR system (Applied Biosystems). The $2^{-\Delta\Delta CT}$ method (Livak and Schmittgen, 2001) was applied for data analysis. Primer sequences were as follows: β-Actin, CTA CAA TGA GCT GCG TGT GGC (forward), CAG GTC CAG ACG CAG GAT GGC (reverse); GRP94, CGT GTG GAG TAG CAA GAC AGA G (forward), CAT AAG TTC CCA ATC CCA CAC AG (reverse); BiP, TCT GGT GAT CAG GAT ACA GGT G (forward), ATG ATT GTC TTT TGT TAG GGG TCG (reverse).

XBP1 mRNA splicing and ATF6 endoproteolysis

XBP1 and β-Actin mRNAs were reverse-transcribed, PCR amplified and separated by gel electrophoresis on a 2% agarose (Genemate-Bioexpress) gel, as in (Calfon et al., 2002). Ethidium bromide (Sigma) stained amplicons were quantified by densitometry using ImageJ software (NIH). An alternative assay for splicing employed a Tomato fluorescent protein reporter, whose expression was under the control of the XBP1 intron, with the DNA binding domain. This reporter was modified from the GFP reporter described in (Rutkowski et al., 2006). Expression of this reporter was scored and analyzed using an Olympus X-81 inverted microscope controlled by the Volocity software (Perkin Elmer). HEK-293 stably expressing HA-tagged ATF6 were analysed by immunoblotting with anti HA-antibody after the cells were stressed with TM and treated with MG132, to block degradation of the ATF6 fragment. The levels of the ATF6 fragment nuclear fractions were enriched as described in (Li et al., 2000).

Metabolic labeling

3T3 cells, untreated or treated with TG for 6 hrs, were starved for 20 min in Met/Cys-free medium, pulsed for 30 min with 88 μCi [^{35}S]Met/Cys per mL and immediately lysed. Lysates were subjected to immunoprecipitation with the monoclonal anti-GRP94, 9G10 (Enzo). Immune complexes were isolated with Protein G-Sepharose (Invitrogen) for 5 hrs. Samples were resolved on 8% acrylamide gels, dried, exposed to a storage phosphor screen, and imaged with a Typhoon phosphorimager. Band intensities were quantified with the ImageQuant software.

C. elegans methods

Wild type (N2) and mutant strains of C. elegans were obtained from the C. elegans Genetics Center (Minneapolis, MN). The strain VC970 contains the *ok1373* allele, a 578bp deletion in the *tag-320* gene on the X chromosome, maintained as a balanced strain across from the szT1 balancer X chromosome. The *tag-320* gene has been renamed pdi-6. For ease of identification,

the *ok1373* allele was crossed to a strain containing an X chromosome-integrated Q40::YFP array, and maintained by picking young heterozygous adults. The UPR reporter strain was constructed by mating *rrf-3(pk1426)* males to SJ4005 hermaphrodites (where the phsp4::GFP transgene was integrated into chromosome V). Genotypes were monitored by the appropriate PCR reactions. Maintenance of strains, feeding RNAi treatments and observation of larvae and adults were all by standard procedures detailed in WormBook (http://www.wormbook.org). Fecundity was assessed by singling individual L4 animals and enumerating their progeny. The fecundity of *rrf-3* animals grown on OP50 E. coli was 55±12. Individual worms mounted on agar pads were imaged with a Zeiss Axiophot and Olimpus FluoView 1000 microscopes using Nomarski and epifluoresence optics.

Gene silencing

Cells were transduced as previously reported ((Eletto et al., 2012) with lentiviruses carrying the following shRNA clones (Mission library, Sigma):

1) shBiP; TRCN0000008455;

5'-CCGGCTCGAATGTAATTGGAATCTTCTCGAGAAGATTCCAATTACATTCGAGTTTTT-3'

2) shGRP94; TRCN0000071925

5'-CCGGGCTATTCAGTTGGATGGGTTACTCGAGTAACCCATCCAACTGAATAGCTTTTTG-3'

3) shPDIA1; TRCN0000111865;

5'-CCGGGCATTTCATCTGTGAGGCATTCTCGAGAATGCCTCACAGATGAAATGCTTTTTG-3'

4) shPDIA6-clone 1; TRCN0000111770

5'-CCGGCTATGAATTGTAGCAGTGAATCTCGAGATTCACTGCTACAATTCATAGTTTTTG-3'

5) shPDIA6-clone 2; TRCN0000111774;

5'- CCGGCGCAAGATGAAATTTGCTCTTCTCGAGAAGAGCAAATTTCATCTTGCGTTTTTG -3'

6) shPDIA6-clone 3; TRCN0000433401

5'-CCGGGTAGTACTTGATTGGTCATTTCTCGAGAAATGACCAATCAAGTACTACTTTTTTG -3'

7) shPDIA3; TRCN0000008451

5'- CCGGGACCAGTTTATGTTTGTGGTTCTCGAGAACCACAAACATAAACTGGTCTTTTT -3'

Immunoblotting, immunoprecipitation and antibodies

For protein determination, cells were washed in ice-cold PBS buffer and lysed in 50mM Tris pH 8; 150mM NaCl; 20mM iodoacetamide; 5mM KCl; 5mM MgCl2; 1% NP-40; supplemented with protease and phosphatase inhibitor cocktails (PhosSTOP™ from Roche). Protein

concentrations were determined with a BCA Assay (Thermo). Immunoblotting was performed using the PPDS module of the Owl Separation System™ (Thermo) and 10% 37.5:1 Acrylamide/Bis-Acrylamide poly-acrylamide gels. SDS-PAGE was performed using Tris-Glycine-SDS buffer and transferred onto 0.45um nitrocellulose membrane (Biorad) in Tris-Glycine buffer plus 20% methanol, using a Genie™ Blot Module (Thermo). Nitrocellulose membranes were blocked in 5% non-fat milk in TBS buffer. For blots to be probed with antibody against phospho-proteins a 1:1 mixture of Odyssey® blocking buffer (Licor) and Tris-buffered saline (TBS) solution was used. The blots were then incubated overnight at 4°C, in 1% non-fat milk/TBS-0.1% Tween (TBS-T) plus the primary antibody. Afterward the membranes were washed in TBS-T and incubated with the appropriate infrared (IR)-labeled secondary antibody (from Licor) in 5% milk/TBS-T. The membranes were washed and scanned using the Odyssey® Infrared Imaging System (Licor). Protein bands were visualized and densitometry determined by the Licor Odyssey software. IRE1 phosphorylation was analyzed by SDS/PAGE in the presence of 25μM Phos-tag reagent (NARD Institute) and 50μM MnCl2 (Yang et al., 2010). Anti-HA affinity agarose beads (clone HA-7, Sigma) were used to immunoprecipitate (IP) HA-tagged IRE1. Anti-V5 Agarose Affinity Gel (V5-10, Sigma) was used for the IP of V5-tagged PDIA6. IP was performed in TNNB buffer (50mM TRIS pH 8, 250mM NaCl, 0.5% NP-40, 0.1% BSA, 0.002% NaN3), at 4°C for 4hr. Beads were washed in TNNB without BSA and protein eluates were analysed by SDS-PAGE. Mouse anti-KDEL (clone 10C4) and rabbit anti-14-3-3 ζ (C-19) antibodies were purchased from Santa Cruz Biotechnology. Rabbit anti-PDIA6, mouse anti-PDIA1 (RL-90) and rabbit anti-OS.9 [EPR4272(2)] antibodies were purchased from Abcam. Mouse anti-V5 and rabbit anti-GFP antibodies were purchased from Invitrogen. Mouse anti-HA.11 (16B12) antibody was purchased from Covance. A rabbit monoclonal anti-HA (Cell Signaling) was used in the ATF6 endoproteolysis analysis. Rabbit anti-IRE1 (14C10), rabbit anti-phospho-JNK (Thr183/Tyr185, 98F2) and rabbit anti-JNK (56G8) antibodies were purchased from Cell Signaling Technology. Mouse anti-BiP antibody was purchased from BD Transduction Laboratories. Rabbit anti-GRP170 was a kind gift from Dr. Linda M. Hendershot (St. Jude Children's Research Hospital). IR secondary antibodies (used at 1:10000 dilutions) were from Licor.

Colony formation Assay

HeLa cells, which form tight, distinct colonies, were used for this protocol, adapted from (Yamamoto et al., 2007). Cells were plated at $5x10^3$ cells/35mm well. 24 hrs later, they were exposed to 50nM TG for the indicated times, then returned to growth medium. After 6 days, cells were stained with 200μl of 0.2% (w/v) crystal violet (Amresco) in 2% ethanol for 10 min at room temperature, washed three times with water, and dried. Stained colonies were photographed, then solubilized with 600 μl of 2% SDS, and absorbance of the resulting solution was measured at 570 nm, using a Synergy HT™ plate reader (Bio-Tek). Cell viability was calculated as a ratio of A570 between untreated and treated cells.

Cell viability assay

293T cells, expressing the indicated shRNA clones and/or DNA plasmids, were plated in 96-well plates (1-5x103 cells/well) in quadruplicate. Cell viability was monitored using XTT [2,3-bis-(2-methoxy-4-nitro-5-sulfophenyl)-2H-tetrazolium-5-carboxanilide] Cell Viability Assay Kit (Biotium), according the manufacturer's instructions.

Luciferase reporter assays

Constructs composed of nucleotides −284 to +221 of the human BiP promoter driving firefly luciferase were described in (Doroudgar et al., 2009). 293T or *IRE1α* $^{-/-}$ or $^{+/+}$ MEFs stably expressing shRNA targeting either PDIA6, BiP or a non-relevant sequence (shCtrl) were transfected and analyzed for luciferase activity as in (Doroudgar et al., 2009). The 5X ATF6 site luciferase reporter was described in (Wang et al., 2000). Firefly luciferase reporters were co-transfected with *Renilla* luciferase (pRL-TK, from Addgene), to normalize for transfection efficiency and protein synthesis.

Statistical and computational analyses

Statistical significance was determined by two-tailed student t test. Sequence alignment was done with the Lalign algorithm. Phylogenetic analysis was generated using Phylogeny.fr (Dereeper et al., 2008).

Supplemental References

Calfon, M., Zeng, H., Urano, F., Till, J.H., Hubbard, S.R., Harding, H.P., Clark, S.G., and Ron, D. (2002). IRE1 couples endoplasmic reticulum load to secretory capacity by processing the XBP-1 mRNA. Nature 415, 92-96.

Dereeper, A., Guignon, V., Blanc, G., Audic, S., Buffet, S., Chevenet, F., Dufayard, J.F., Guindon, S., Lefort, V., Lescot, M., et al. (2008). Phylogeny.fr: robust phylogenetic analysis for the non-specialist. Nucleic Acids Res 36, W465-469.

Doroudgar, S., Thuerauf, D.J., Marcinko, M.C., Belmont, P.J., and Glembotski, C.C. (2009). Ischemia activates the ATF6 branch of the endoplasmic reticulum stress response. J Biol Chem 284, 29735-29745.

Eletto, D., Maganty, A., Eletto, D., Dersh, D., Makarewich, C., Biswas, C., Doroudgar, S., Glembotski, C.C., and Argon, Y. (2012). Limitation of Individual Folding Resources in the ER Leads to Outcomes Distinct from the Unfolded Protein Response. Journal of Cell Science 125, 4865-4875.

Han, D., Lerner, A.G., Vande Walle, L., Upton, J.P., Xu, W., Hagen, A., Backes, B.J., Oakes, S.A., and Papa, F.R. (2009). IRE1alpha kinase activation modes control alternate endoribonuclease outputs to determine divergent cell fates. Cell 138, 562-575.

Hartley, T., Siva, M., Lai, E., Teodoro, T., Zhang, L., and Volchuk, A. (2010). Endoplasmic reticulum stress response in an INS-1 pancreatic beta-cell line with inducible expression of a folding-deficient proinsulin. BMC Cell Biol 11, 59.

Li, M., Baumeister, P., Roy, B., Phan, T., Foti, D., Luo, S., and Lee, A.S. (2000). ATF6 as a transcription activator of the endoplasmic reticulum stress element: thapsigargin stress-induced changes and synergistic interactions with NF-Y and YY1. Mol Cell Biol 20, 5096-5106.

Livak, K.J., and Schmittgen, T.D. (2001). Analysis of relative gene expression data using real-time quantitative PCR and the 2(-Delta Delta C(T)) Method. Methods 25, 402-408.

Rutkowski, D.T., Arnold, S.M., Miller, C.N., Wu, J., Li, J., Gunnison, K.M., Mori, K., Sadighi Akha, A.A., Raden, D., and Kaufman, R.J. (2006). Adaptation to ER stress is mediated by differential stabilities of pro-survival and pro-apoptotic mRNAs and proteins. PLoS Biol 4, e374.

Urano, F., Wang, X., Bertolotti, A., Zhang, Y., Chung, P., Harding, H.P., and Ron, D. (2000). Coupling of stress in the ER to activation of JNK protein kinases by transmembrane protein kinase IRE1. Science 287, 664-666.

Wang, Y., Shen, J., Arenzana, N., Tirasophon, W., Kaufman, R.J., and Prywes, R. (2000). Activation of ATF6 and an ATF6 DNA binding site by the endoplasmic reticulum stress response. J Biol Chem 275, 27013-27020.

Yamamoto, K., Sato, T., Matsui, T., Sato, M., Okada, T., Yoshida, H., Harada, A., and Mori, K. (2007). Transcriptional induction of mammalian ER quality control proteins is mediated by single or combined action of ATF6alpha and XBP1. Dev Cell 13, 365-376.

Yang, L., Xue, Z., He, Y., Sun, S., Chen, H., and Qi, L. (2010). A Phos-tag-based approach reveals the extent of physiological endoplasmic reticulum stress. PLoS One 5, e11621.